Activation Energies of Pericyclic Reactions: Performance of DFT, MP2, and CBS-QB3 Methods for the Prediction of Activation Barriers and Reaction Energetics of 1,3-Dipolar Cycloadditions, and Revised Activation Enthalpies for a Standard Set of Hydrocarbon Pericyclic Reactions

Daniel H. Ess and K. N. Houk*

Department of Chemistry and Biochemistry, University of California, Los Angeles, California 90095-1569

Received: May 12, 2005

Activation barriers and reaction energetics for the three main classes of 1,3-dipolar cycloadditions, including nine different reactions, were evaluated with the MPW1K and B3LYP density functional methods, MP2, and the multicomponent CBS-QB3 method. The CBS-QB3 values were used as standards for 1,3-dipolar cycloaddition activation barriers and reaction energetics, and the density functional theory (DFT) and MP2 methods were benchmarked against these values. The MPW1K/6-31G* method and basis set performs best for activation barriers, with a mean absolute deviation (MAD) value of 1.1 kcal/mol. The B3LYP/6-31G* method and basis set performs best for reaction enthalpies, with a MAD value of 2.4 kcal/mol, while the MPW1K method shows large errors for reaction energetics. The MP2 method gives the expected systematic underestimation of barriers. Concerted and nearly synchronous transition structures are predicted by all DFT and MP2 methods. Also reported are revised estimated 0 K experimental activation enthalpies for a standard set of hydrocarbon pericyclic reactions and updated comparisons to experiment for DFT, ab initio, and multicomponent methods. B3LYP and MPW1K methods with MAD values of 1.5 and 2.1 kcal/mol, respectively, fortuitously outperform the multicomponent CBS-QB3 method, which has a MAD value of 2.3. The MAD value of the O3LYP functional improves to 2.4 kcal/mol from the previously reported 3.0 kcal/mol.

Introduction

Over the past decade compound quantum mechanical methods capable of producing chemically accurate (±1 kcal/mol) thermodynamic values have been developed and refined.[1] Most notable is the G-series developed by Pople et al.,[2−5] the CBS series by Petersson et al.,[6−11] and the W-series by Martin et al.[12] Hybrid density functional theory (DFT) methods are widely used due to the balance between speed and accuracy. To approach the accuracy of compound methods, development of more accurate DFT methods have been undertaken by many groups.[13−15] These DFT functionals have been parametrized and tested for groups of standard reactions.

Guner et al. previously reported a comparison of different levels of theory for hydrocarbon pericyclic reactions. Revised estimated 0 K experimental activation enthalpies for these pericyclic reactions and updated comparisons to experiment for DFT, ab initio, and multicomponent methods are included at the end of this paper.[16,17] We now report the performance of different methods and basis sets for the prediction of activation barriers and reaction energetics for the three most important classes of 1,3-dipolar cycloadditions involving zwitterionic heteroatom-containing molecules.[18−21] The cycloadditions of ethylene and acetylene with the parent diazonium, nitrilium, and azomethine betaine classes of 1,3-dipoles (Figure 1) were studied.[22] CBS-QB3 activation barriers and reaction energetics were obtained for these classes of dipolar cycloadditions, which can be used in the future to benchmark new methods. The results

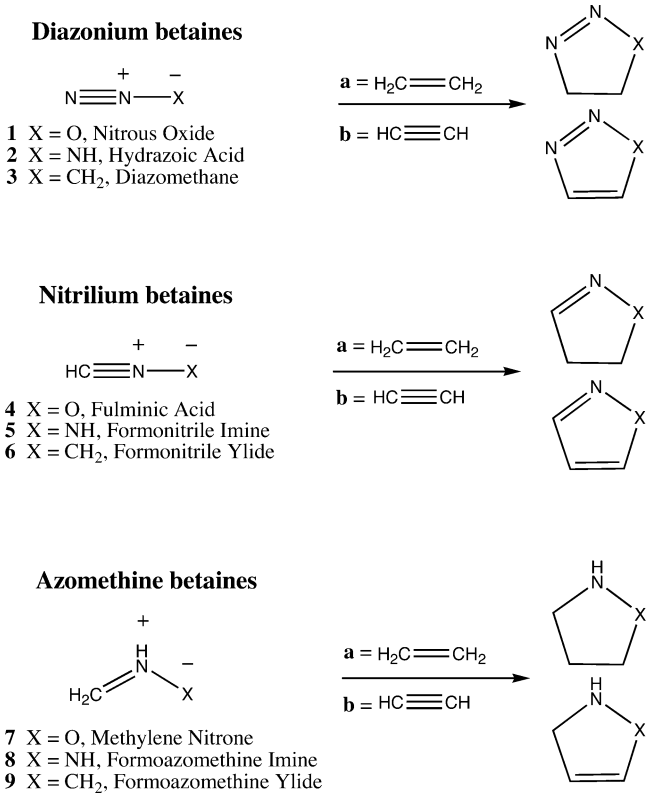

Figure 1. Classes of 1,3-dipolar cycloaddition reactions studied in this work.

* Corresponding author. E-mail: houk@chem.ucla.edu.

10.1021/jp052504v CCC: $30.25
Published on Web 10/05/2005

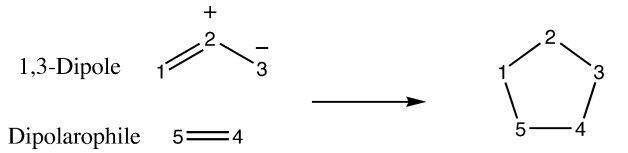

Figure 2. The 1,3-dipolar cycloaddition.

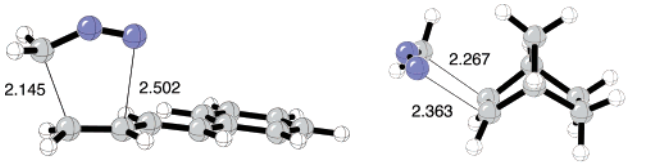

Experimental[27] = 13.8 ± 0.8
CBS-QB3 = 13.0
B3LYP/6-31G* = 16.1
MPW1K/6-31G* = 16.0

Experimental[63] = 13.2 ± 0.9
CBS-QB3 = 10.4
B3LYP/6-31G* = 15.8
MPW1K/6-31G* = 15.6

Figure 3. Activation enthalpies at 298 K for reactions of diazomethane with 1-phenylbutadiene and norbornene. The CBS-QB3, B3LYP, and MPW1K methods are compared relative to the experimental values.

of calculations with the B3LYP and MPW1K DFT methods, and MP2, were also compared to the CBS-QB3 results.

The 1,3-dipolar cycloaddition reaction was defined and developed experimentally into a general and highly useful synthetic method through a series of classic studies by Rolf Huisgen and his group in the 1960s.[22−27] There have been many experimental and theoretical studies of 1,3-dipolar cycloadditions.[22−42] The general 1,3-dipolar cycloaddition, shown in Figure 2, is the union of a 1,3-dipole with a dipolarophile forming two new sigma bonds. The dipolarophile is an unsaturated hydrocarbon or heteroatomic derivative. Control of regioselectivity of 1,3-dipolar cycloadditions has been explained by frontier molecular orbital (FMO) analysis.[34] The nucleophilicity and electrophilicity of the dipole and dipolarophile are based on HOMO and LUMO energies and orbital coefficients in this treatment.[28−35,40−42]

A 1,3-dipole is a molecule that has zwitterionic (dipolar) all-octet resonance structure and adds 1,3 in cycloadditions. Huisgen defined the classes of 1,3-dipoles.[22] The three most important, studied here, are the diazonium, nitrilium, and azomethine betaine classes shown in Figure 1. Ozone, carbonyl betaines, and a variety of other heterosubstituted species are also 1,3-dipoles. There have been discussions of the diradical character of 1,3-dipoles.[43−46] Diradical character does not, however, necessarily predispose the cycloaddition to a stepwise diradical mechanism, and concerted versus stepwise diradical cycloaddition mechanisms have been debated in the literature.[25,47] Previous calculations provide evidence that 1,3-dipolar cycloadditions proceed through a concerted, but often asynchronous reaction mechanism.[35] There is some evidence that a few reactions proceed through a stepwise diradical intermediate mechanism.[47−50] Early computational work reveled a systematic difference between semiempirical and ab initio methods for computing transition structure geometries. Ab initio methods showed a preference for synchronous transition structures, while semiempirical methods computed very asynchronous structures.[37] At the time, neither approach properly accounted for electron correlation, and so the definitive conclusion about the nature of the transition structure could not be made. Here we survey DFT methods for computing 1,3-dipolar cycloaddition activation and reaction enthalpies by comparing them to the CBS-QB3 method, which is expected to give accurate results, based upon previous comparisons with experimental data.

TABLE 1: CBS-QB3, B3LYP, MPW1K, and MP2 Computed Enthalpies of Activation ($\Delta H^{\ddagger}_{0K}$) and Enthalpies of Reaction ($\Delta H_{rxn,0K}$), Except with MP2, at 0 K for Eighteen Parent 1,3-Dipolar Cycloaddition Reactions (1a−9b)

method		1a	1b	2a	2b	3a	3b	4a	4b	5a	5b	6a	6b	7a	7b	8a	8b	9a	9b
CBS-QB3	$\Delta H^{\ddagger}$	27.9	27.9	20.3	20.1	14.6	15.2	13.0	14.1	7.2	8.5	5.9	7.4	13.8	14.0	6.6	8.1	0.9	1.5
	ΔH_{rxn}	−4.4	−37.1	−19.7	−61.5	−31.7	−49.0	−39.3	−74.0	−57.4	−100.3	−68.0	−86.7	−28.8	−43.9	−42.8	−60.8	−62.7	−76.9
B3LYP/6-31G*	$\Delta H^{\ddagger}$	25.1	24.5	19.5	18.6	16.6	16.4	13.3	13.7	8.7	9.1	8.8	10.6	13.7	13.0	6.9	8.5	3.5	3.6
	ΔH_{rxn}	−6.7	−43.9	−20.2	−64.9	−30.6	−51.4	−39.8	−79.0	−55.6	−102.0	−65.1	−87.6	−28.7	−48.1	−41.8	−64.8	−61.2	−79.2
B3LYP/6-31+G**	$\Delta H^{\ddagger}$	26.3	25.9	20.6	19.5	18.2	17.7	14.8	15.1	10.0	10.3	10.7	11.1	16.8	15.8	10.4	10.8	6.1	5.6
	ΔH_{rxn}	−4.4	−40.7	−17.8	−62.4	−27.0	−48.0	−36.1	−74.4	−52.1	−98.6	−60.1	−82.9	−22.2	−41.5	−35.8	−59.0	−54.3	−72.8
B3LYP/6-31+G(2d,p)	$\Delta H^{\ddagger}$	27.7	27.1	21.6	20.5	18.1	17.6	15.2	15.4	10.4	10.6	10.5	10.9	17.2	16.1	11.1	11.2	6.1	5.4
	ΔH_{rxn}	−2.7	−38.5	−16.8	−60.7	−27.2	−47.9	−35.1	−73.0	−51.5	−97.2	−60.2	−82.5	−21.8	−40.8	−35.4	−58.1	−54.4	−72.8
B3LYP/6-311+G(2d,p)	$\Delta H^{\ddagger}$	29.3	28.8	23.5	22.5	19.6	19.1	16.7	17.2	11.4	11.8	10.9	11.5	18.0	17.2	12.0	12.1	−4.9	−5.4
	ΔH_{rxn}	0.0	−34.7	−13.0	−55.8	−23.5	−43.2	−32.2	−68.9	−48.5	−93.1	−57.9	−79.2	−20.1	−38.3	−33.2	−55.2	−63.6	−81.2
MPW1K/6-31G*	$\Delta H^{\ddagger}$	27.6	27.7	20.3	20.2	16.2	16.6	15.0	16.0	8.3	9.3	7.7	9.1	12.3	12.2	4.4	6.8	1.2	1.7
	ΔH_{rxn}	−16.4	−53.3	−33.7	−79.7	−44.8	−65.1	−53.1	−92.3	−99.6	−120.5	−82.6	−104.4	−43.3	−61.4	−59.3	−81.6	−79.8	−97.0
MPW1K/6-31+G**	$\Delta H^{\ddagger}$	28.6	28.7	21.3	21.0	17.6	17.7	16.1	17.1	9.3	10.2	9.1	10.2	14.7	14.3	7.3	8.5	3.1	3.2
	ΔH_{rxn}	−14.6	−51.0	−31.7	−77.8	−41.8	−62.4	−50.0	−88.8	−98.8	−117.8	−78.4	−100.5	−37.9	−56.2	−54.3	−76.9	−73.6	−91.6
MPW1K/6-311+G(2d,p)	$\Delta H^{\ddagger}$	31.6	31.5	24.2	23.7	18.9	18.8	17.9	18.8	10.8	11.6	9.4	10.4	16.0	15.5	8.8	9.6	3.5	3.5
	ΔH_{rxn}	−28.2	−45.7	−27.5	−71.9	−39.2	−58.9	−47.1	−84.4	−97.3	−113.0	−77.0	−98.1	−36.4	−53.9	−52.1	−73.9	−72.1	−89.5
MP2(Full)/6-31G*	$\Delta H^{\ddagger}$	28.8	30.2	16.9	18.3	8.5	10.3	10.6	12.2	1.9	3.8	1.0	3.1	10.1	11.8	0.6	5.8		0.6

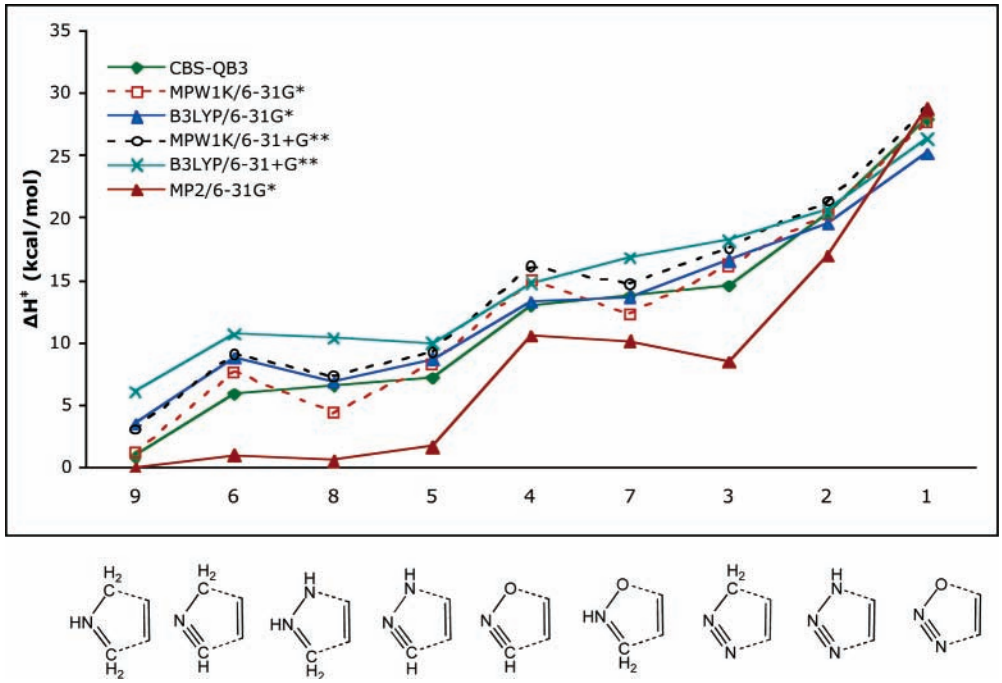

Figure 4. Comparisons of DFT and ab initio methods and basis sets for reactions of nine 1,3-dipoles with ethylene.

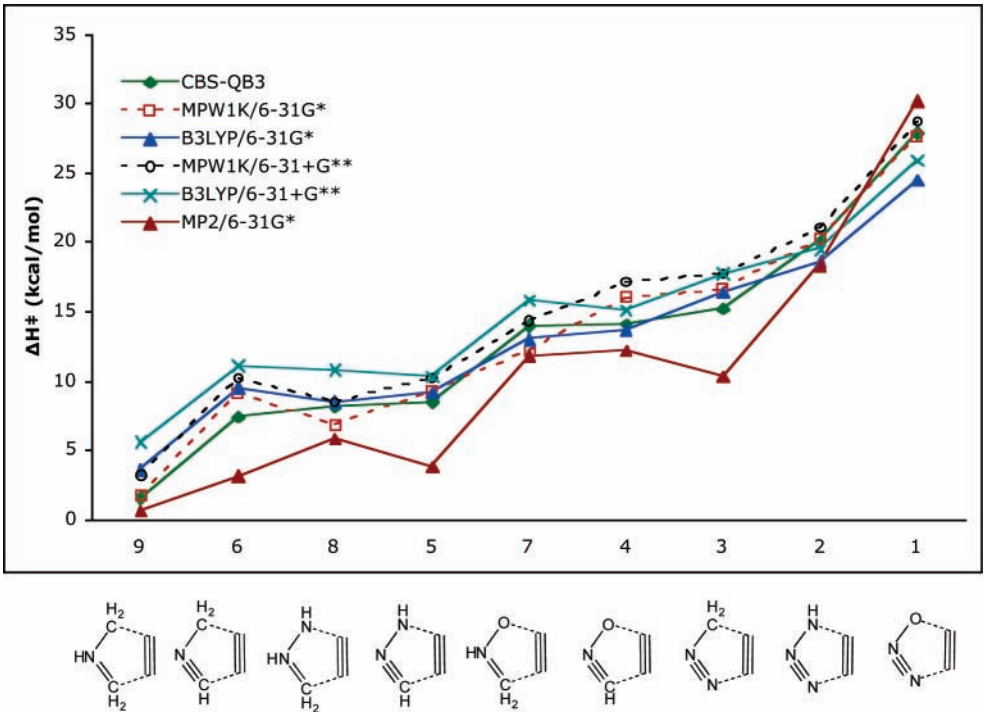

Figure 5. Comparisons of DFT and ab initio methods and basis sets for reactions of nine 1,3-dipoles with acetylene.

Computational Methods

The so-called "semiempirical nature" of DFT methods results from the unknown exchange-correlation functional in the Kohn−Sham equations. The terms are estimated by exchange-correlation functionals plus varying amounts of Hartree−Fock (HF) exact exchange in hybrid DFT theory. Becke implemented this approach based on the adiabatic connection theory, which connects the fully correlated system to the Kohn−Sham non-interacting system.[51,52]

The B3LYP method uses this hybrid approach with an exact HF exchange term, local spin density exchange term (LSDA), Becke's 1988 gradient correction to the LSDA exchange, and, for correlation, the Lee−Yang−Parr correlation functional and the VWN local correlation expression (eq 1).[53,54]

$$E_{xc} = (1 - a_0)E_x^{LSDA} + a_0E_x^{HF} + a_x\Delta E_x^{88} + a_cE_c^{LYP} + (1 - a_0)E_c^{VWN} \quad (1)$$

$$a_0 = 0.2, \qquad a_x = 0.72, \qquad a_c = 0.81$$

Another hybrid method similar to B3LYP is the *m*PW1PW91 method which uses the modified Perdew−Wang (*m*PW) gradient-corrected exchange functional, 25% Hartree−Fock exchange, and the Perdew−Wang gradient-corrected correlation

TABLE 2: Mean Deviations (MD), Mean Absolute Deviations (MAD), Standard Deviations (SD) of the MAD, and Maximum Negative and Positive Errors Relative to CBS-QB3 Computed Enthalpies of Activation for Eighteen 1,3-Dipolar Cycloadditions (kcal/mol)

method	MD	MAD	SD	max (−) error	max (+) error
B3LYP/6-31G*	0.3	1.5	1.0	−3.4[b]	3.2[c]
B3LYP/6-31+G**	2.7	2.6	1.3	−2.0[b]	5.2[e]
B3LYP/6-31+G(2d,p)	2.5	2.6	1.5	−0.8[b]	5.1[e]
B3LYP/6-311+G(2d,p)	2.5	3.9	1.5	−6.9[c]	5.4[d]
MPW1K/6-31G*	0.3	1.1	0.8	−2.2[d]	1.9[f]
MPW1K/6-31+G**	1.7	1.7	1.0	*a*	3.1[f]
MPW1K/6-311+G(2d,p)	3.2	3.2	1.0	*a*	4.9[f]
MP2/6-31G*	−3.0	3.4	1.7	−6.1[g]	2.4[b]

[a] None of the computed activation enthalpies were lower than the CBS-QB3 value. [b] Nitrous oxide with acetylene. [c] Formoazomethine ylide with acetylene. [d] Formoazomethine imine with ethylene. [e] Formoazomethine ylide with ethylene. [f] Fulminic acid with ethylene. [g] Diazomethane with ethylene.

TABLE 3: Mean Deviations (MD), Mean Absolute Deviations (MAD), Standard Deviations (SD) of the MAD, and Maximum Negative and Positive Errors Relative to CBS-QB3 Computed Enthalpies of Reaction for Eighteen 1,3-Dipolar Cycloadditions (kcal/mol)

method	MD	MAD	SD	max (−) error	max (+) error
B3LYP/6-31G*	−1.4	2.4	1.7	−6.7[b]	2.9[e]
B3LYP/6-31+G**	3.0	3.6	2.6	−3.6[c]	8.4[f]
B3LYP/6-31+G(2d,p)	3.8	4.0	2.5	−1.4[b]	8.3[f]
B3LYP/6-311+G(2d,p)	5.7	6.3	2.4	−4.3[c]	10.1[e]
MPW1K/6-31G*	−17.9	17.9	6.6	−42.2[d]	*a*
MPW1K/6-31+G**	−14.4	14.4	7.2	−41.4[d]	*a*
MPW1K/6-311+G(2d,p)	−12.3	12.3	7.8	−40.0[d]	*a*

[a] None of the computed reaction enthalpies were less exothermic than the CBS-QB3 value. [b] Nitrous oxide with acetylene. [c] Formoazomethine ylide with acetylene. [d] Formonitrile imine with ethylene. [e] Formonitrile ylide with ethylene. [f] Formoazomethine ylide with ethylene.

functional (PW91).[55] Truhlar found that increasing the HF exchange fraction from 0.25 to 0.428 gave a method that is more accurate for barrier heights.[56] This modified Perdew−Wang one-parameter model for kinetics (MPW1K) was optimized against 20 barrier heights. This method performed better than ab initio and multicoefficient correlation methods for hydrogen abstractions. The 6-31+G** basis set was recommended.[56−60]

The CBS methods were developed with the idea that a major source of error in quantum mechanical calculations arises from truncation of the basis set.[6] The complete basis set (CBS) models are compound methods that extrapolate to the CBS limit by using a N^{-1} asymptotic convergence of MP2 pair energies calculated from pair natural orbital expansions.[6−11] CBS-QB3 uses the B3LYP method for geometry and frequencies. This highly accurate method is a five-step method starting with a B3LYP/6-311G(2d,d,p) geometry and frequency calculation, followed by CCSD(T), MP4SDQ, and MP2 single-point calculations and a CBS extrapolation.[6]

All optimizations using the MPW1K density functional were performed using the Gaussian 98 suite of programs.[61] CBS-QB3 reactant and product optimizations were performed using Gaussian 98, while CBS-QB3, MP2, and some B3LYP transition structure optimizations were performed using Gaussian 03.[62]

Frequency calculations were used to characterize all optimizations as minima or first-order saddle points. All reaction and activation enthalpies reported were zero-point-energy (ZPE) corrected, but with no thermal corrections; they are, therefore, $\Delta H_{(0K)}$. Activation barriers compare transition structure energies to reactants. The ZPEs were not scaled. Stable calculations were performed for all optimized reactants, products, and transition structures with the 6-31G* and 6-311+G(2d,p) basis sets for B3LYP and MPW1K methods, to verify that open-shell func-

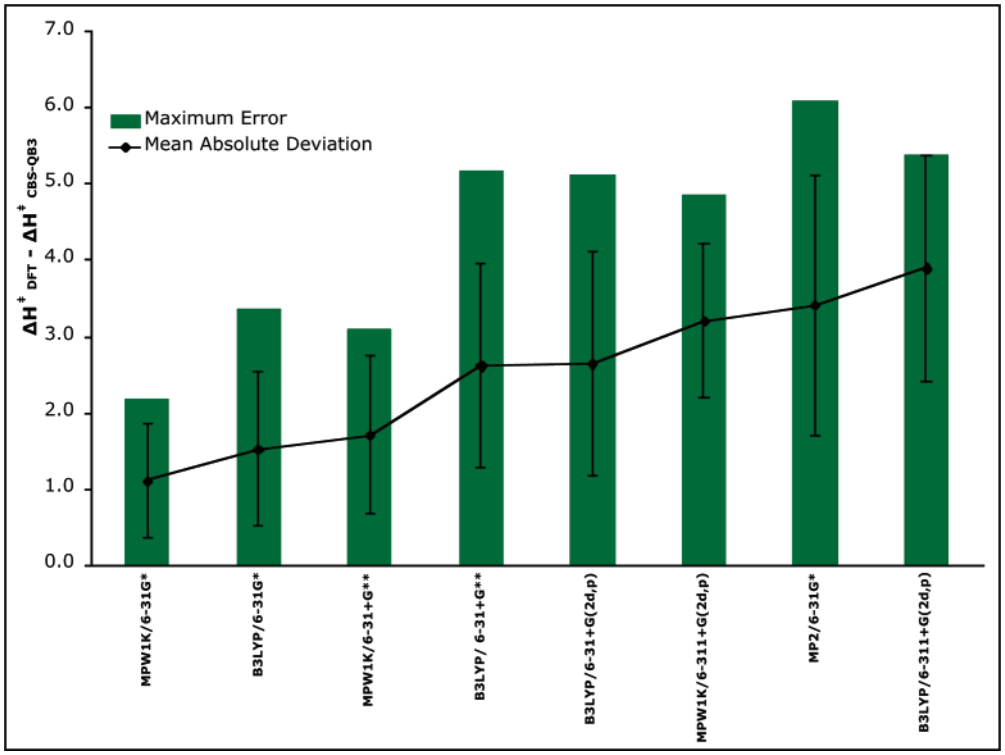

Figure 6. Mean absolute deviations of B3LYP and MPW1K activation enthalpies from the computed CBS-QB3 activation enthalpy values. Green bars represent maximum absolute error. Error bars show standard deviations of the MAD values.

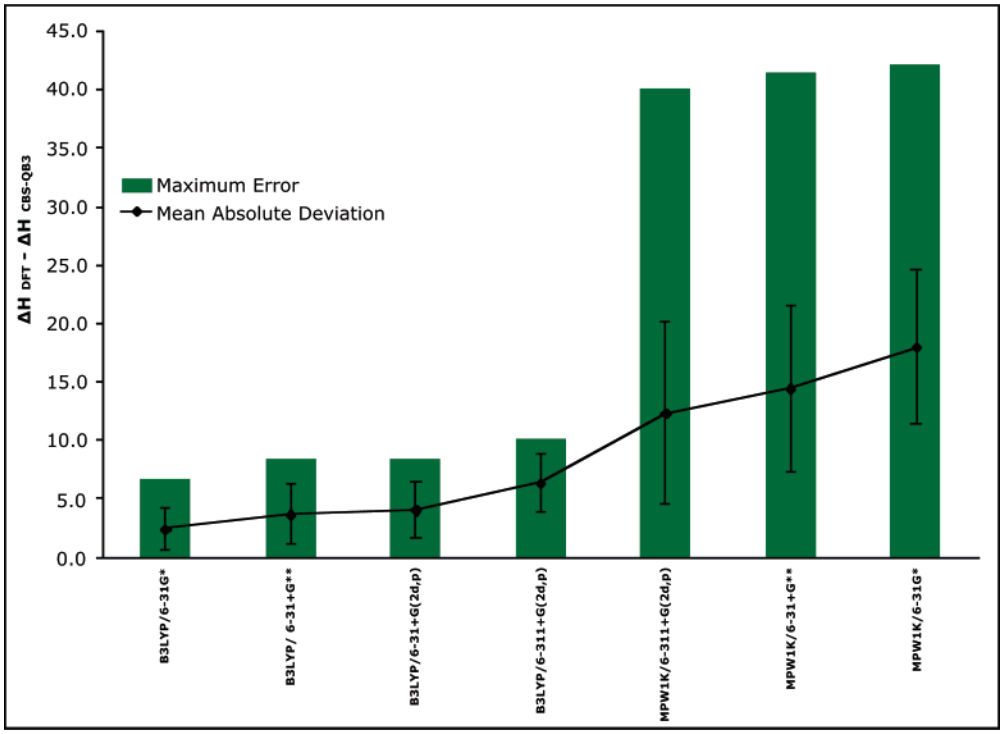

Figure 7. Mean absolute deviation of B3LYP and MPW1K reaction enthalpies from the computed CBS-QB3 reaction enthalpy values. Green bars represent maximum absolute error. Error bars show standard deviations of the MAD values.

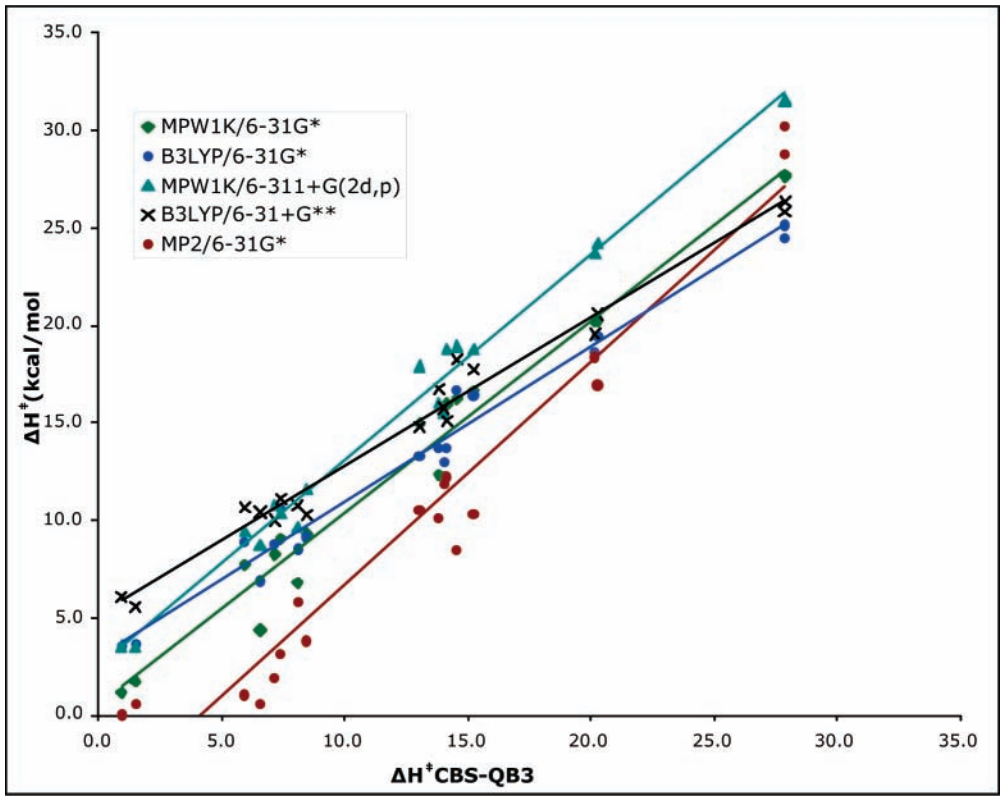

Figure 8. Plot of computed activation enthalpies at 0 K vs CBS-QB3 activation enthalpies at 0 K for reactions **1**−**9**. A linear regression is also plotted. MPW1K/6-31G*: $y = 0.984x + 0.502$, $R^2 = 0.971$. B3LYP/6-31G*: $y = 0.795x + 2.981$, $R^2 = 0.976$. MPW1K/6-311+G(2d,p): $y = 1.055x + 2.502$, $R^2 = 0.988$. B3LYP/6-31+G**: $y = 0.758x + 5.199$, $R^2 = 0.980$. MP2/6-31G*: $y = 1.141x - 4.699$, $R^2 = 0.9495$. $N = 18$ for all linear regressions.

tions were not more stable. Open-shell transition structures were computed using UB3LYP/6-31G* for the 18 parent reactions, but in all cases it was found that open-shell functions were not more stable than closed-shell functions.

Results and Discussion

The performance of the CBS-QB3 standard was evaluated earlier by Guner et al. for a set of 11 pericyclic reactions. The

TABLE 4: Statistical Values Comparing the B3LYP and MPW1K Methods Relative to CBS-QB3 Computed Activation Enthalpies for Three Classes of 1,3-Dipolar Cycloadditions (kcal/mol)

method	MD	MAD	SD	max (−) error	max (+) error
		Diazonium Betaines			
B3LYP	−0.9	2.0	1.0	−3.4	2.1
MPW1K	0.4	0.6	0.7	−0.3	1.7
		Nitrilium Betaines			
B3LYP	−1.4	3.7	5.5	−0.5	3.2
MPW1K	−3.4	6.1	10.9	*a*	1.9
		Azomethine Betaines			
B3LYP	0.7	1.1	1.0	−1.1	2.6
MPW1K	−1.1	1.2	0.8	−2.2	0.2

[a] None of the computed activation enthalpies were lower than the CBS-QB3 value. B3LYP and MPW1K were compared with the 6-31G* basis set.

TABLE 5: Statistical Values Comparing the B3LYP and MPW1K Methods Relative to CBS-QB3 Computed Activation and Reaction Enthalpies at 0 K for Oxide, Imine, and Ylide 1,3-Dipolar Cycloadditions (kcal/mol)

method		MD	MAD	SD	max (−) error	max (+) error
			Oxides			
B3LYP	$\Delta H^{\ddagger}$	−1.3	1.3	1.4	−3.4	0.3
	ΔH_{rxn}	−3.1	3.2	2.6	−6.7	0.1
MPW1K	$\Delta H^{\ddagger}$	0.0	1.3	0.8	−1.8	1.9
	ΔH_{rxn}	−15.4	15.4	2.4	−18.4	*b*
			Imines			
B3LYP	$\Delta H^{\ddagger}$	0.1	0.9	0.6	−1.6	1.6
	ΔH_{rxn}	−1.1	2.1	1.3	−4.0	1.8
MPW1K	$\Delta H^{\ddagger}$	−0.3	0.9	0.8	−2.2	1.1
	ΔH_{rxn}	−22.0	22.0	10.2	−42.2	*b*
			Ylides			
B3LYP	$\Delta H^{\ddagger}$	2.3	2.3	0.7	*a*	3.2
	ΔH_{rxn}	0.0	1.9	0.8	−2.4	2.9
MPW1K	$\Delta H^{\ddagger}$	1.2	1.2	0.7	*a*	1.8
	ΔH_{rxn}	−16.4	16.4	2.4	−20.1	*b*

[a] None of the computed activation enthalpies were lower than the CBS-QB3 value. [b] None of the computed reaction enthalpies were less exothermic than the CBS-QB3 value. Oxide reactions (**1**, **4**, and **7**). Imine reactions (**2**, **5**, and **8**). Ylide reactions (**3**, **6**, and **9**). B3LYP and MPW1K were compared with the 6-31G* basis set.

CBS-QB3 method was found to have a mean absolute deviation (MAD) value of 1.9 and standard deviation (SD) of 1.6 when compared to experimental activation enthalpies for these pericyclic reactions.[16,17] CBS-QB3, CASPT2, and B3LYP methods performed best compared to MPW1K, KMLYP, O3LYP, BPW91, MP2, CASSCF, and Hartree−Fock methods.

In the case of 1,3-dipolar cycloadditions, no experimental activation barriers are available for the parent systems. We begin, therefore, by comparing the computed barriers by several methods to barriers measured experimentally for two substituted cases. Transition structures and energetics for the reactions of diazomethane with 1-phenylbutadiene and norbornene are given in Figure 3 and are compared to experimental data. The experimental activation enthalpies are 13.8 ± 0.8 and 13.2 ± 0.9 kcal/mol.[27,63] The computed CBS-QB3 $\Delta H^{\ddagger}_{298K}$ value for the cycloaddition of diazomethane with 1-phenylbutadiene is 13.0 kcal/mol, in agreement with the experimental value. The B3LYP and MPW1K results are too high by more than 2 kcal/mol.

The computed $\Delta H^{\ddagger}_{298K}$ values for the cycloaddition of diazomethane with norbornene are also shown in Figure 3. Here the CBS value is about 3 kcal/mol too low, while the DFT values are 2 kcal/mol too high. As with the reaction with 1-phenylbutadiene, CBS-QB3 predicts the lower activation barrier, while the DFT barrier is predicted to be too high. In this study, we take the CBS-QB3 model to be the most chemically accurate method for barrier heights and reaction energetics, and we evaluate everything in comparison to this standard.

The CBS-QB3, B3LYP, MPW1K, and MP2/6-31G* computed enthalpies of activation ($\Delta H^{\ddagger}_{0K}$) and reaction ($\Delta H_{rxn,0K}$) at 0 K for reactions **1**−**9** are summarized in Table 1. The 6-31G*, 6-31+G**, 6-31+G(2d,p), and 6-311+G(2d,p) basis sets were used for the B3LYP method, and all but the third of these was used for the MPW1K method.

The $\Delta H^{\ddagger}$ values for each method and basis set are plotted for ethylene and acetylene in Figures 4 and 5, respectively. Table 2 lists the overall mean deviations (MD), mean absolute deviations (MAD), standard deviations (SD) of the MAD, and the maximum errors (negative and positive) relative to the corresponding CBS-QB3 calculated enthalpies of activation for each method and basis set for these reactions. The same statistical assessment is shown for the enthalpies of reaction in Table 3. Deviations of MP2 and DFT methods compared to CBS-QB3 are plotted in increasing order of deviation for $\Delta H^{\ddagger}$ and ΔH_{rxn} in Figures 6 and 7.

The MPW1K/6-31G* method and basis set performed best for activation enthalpies giving a MAD value of 1.1 kcal/mol. The B3LYP method using the same basis set had a MAD 0.4 kcal/mol higher than MPW1K. Surprisingly, increasing the size of basis set decreases the accuracy of both MPW1K and B3LYP results, as shown by the increasing MAD and SD values. The MPW1K method tends to overestimate the enthalpy of activation.

The activation barriers computed by the second-order Møller−Plesset perturbation method, which introduces electron correlation through post Hartree−Fock perturbation, are worse than those by all DFT methods, due to a systematic underestimation of all the barriers. The MP2(Full)/6-31G* method and basis set had a MD value of −3.0 and a MAD value of 3.4 kcal/mol. This is 2.4 kcal/mol higher than the best DFT method. This is in agreement with findings of Lynch and Truhlar, who found that DFT methods, especially MPW1K, performed better than MP2 for activation barriers.[64,65,58]

The MPW1K method performed very poorly for reaction enthalpies, and gave values much more exothermic than the CBS-QB3 method. The B3LYP method slightly underestimates reaction enthalpies. All methods and basis sets have larger MAD and SD values for enthalpies of reaction than for enthalpies of activation. B3LYP/6-31G* performs best with a MAD of 2.4 and SD of 1.7. Larger basis sets cause reaction enthalpies to be predicted less accurately, indicated by the steadily increasing MAD and SD values.

Figure 8 is a plot of the MP2 and most accurate DFT methods against the CBS-QB3 activation enthalpy values. Perfect correlation with CBS-QB3 values would result in a line with slope of 1. Linear regression was performed on these plots, and in the caption are the statistical R^2 values and the linear regression functions. With a slope of 0.984 and intercept of 0.502, this type of analysis also showed that MPW1K/6-31G* predicted the most accurate barriers. Even though B3LYP/6-31G* has similar MAD and MD values, with a slope of 0.795, intercept of 2.981, and good linear correlation, this method showed a systematic error, overestimating the barriers. The MP2/6-31G* method underestimated the barriers, and as previously noted

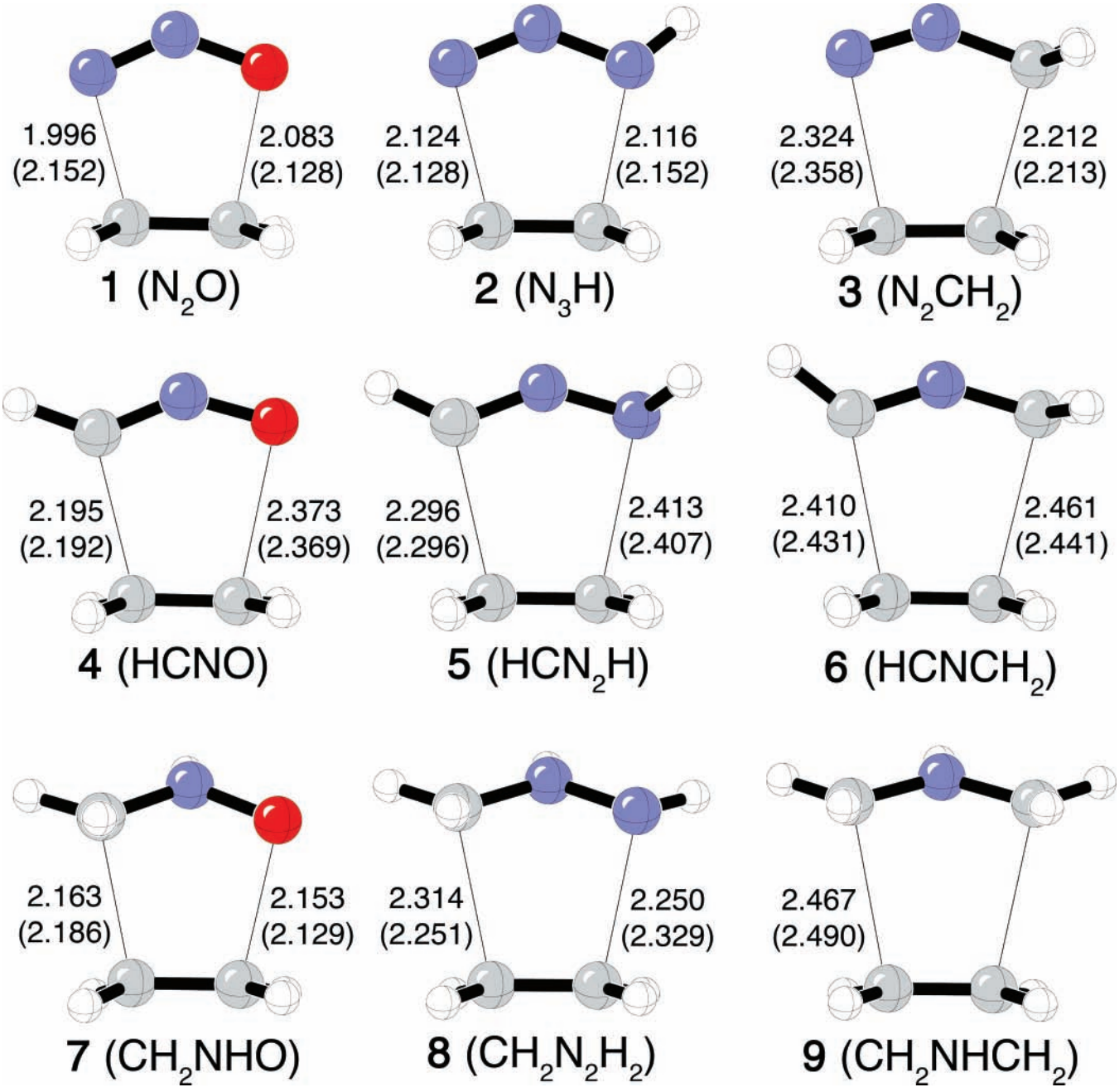

Figure 9. CBS-QB3 (B3LYP/6-311G(2d,d,p)) transition structures for reactions **1a**−**9a** (in parentheses are the partial bond lengths for reactions **1b**−**9b**). **1**, nitrous oxide (N_2O); **2**, hydrazoic acid (N_3H); **3**, diazomethane (N_2CH_2); **4**, fulminic acid (HCNO). **5**, formonitrile imine (HCN_2H); **6**, formonitrile ylide ($HCNCH_2$); **7**, methylene nitrone (CH_2NHO); **8**, formoazomethine imine ($CH_2N_2H_2$); **9**, formoazomethine ylide (CH_2NHCH_2).

MP2 gave a negative MD, but the R^2 value is lower for the DFT methods.

A statistical comparison of $\Delta H^{\ddagger}_{0K}$ values for each class of dipolar cycloaddition is shown in Table 4. A similar comparison for $\Delta H^{\ddagger}_{0K}$ and $\Delta H_{rxn,0K}$ values comparing oxide, imine, and ylide reactions is shown in Table 5. MPW1K predicted barriers much closer to CBS-QB3 than B3LYP when comparing each class of dipolar cycloaddition. However, B3LYP and MPW1K predicted barriers with equal accuracy when compared by type of reaction (oxide, imine, ylide).

The B3LYP/6-311G(2d,d,p) transition structures used for the CBS-QB3 energy evaluations, for reactions **1**−**9** with ethylene, are shown in Figure 9. Partial bond lengths for transition structures of reactions **1**−**9** with acetylene are shown in parentheses. All methods computed concerted synchronous transition structures. The average difference in partial bond length for the B3LYP/6-311G(2d,d,p) method was 0.07 Å. As a comparison of methods for computing transition structure geometries, we compared the 33 different partial bond lengths by plotting each relative to the B3LYP/6-31G* bond length. Figure 10 plots the B3LYP/6-311G(2d,d,p), MPW1K/6-31G*, and MP2/6-31G* partial bond lengths compared to B3LYP/6-31G*. A linear regression analysis shows that the MPW1K method performed best with a slope of 0.994, but the R^2 value of 0.951 is slightly lower than 0.983 for the B3LYP/6-311G-(2d,d,p) method. As can be seen by inspection of Figure 10, the MP2 method varies substantially more than B3LYP/6-311G-

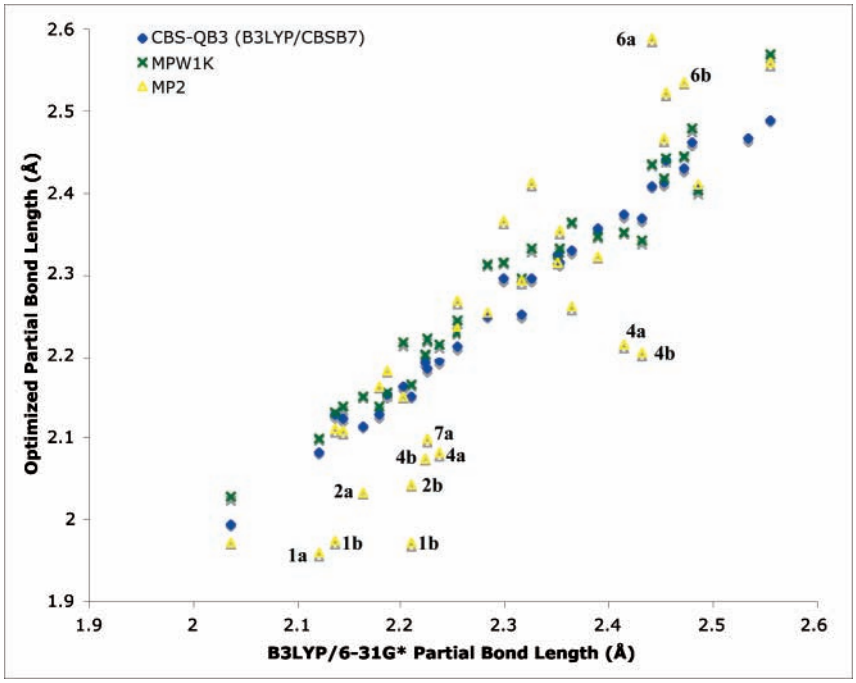

Figure 10. CBS-QB3 (B3LYP/6-311G(2d,d,p)), MPW1K, and MP2(Full) partial bond lengths for reactions **1**−**9** compared to B3LYP. B3LYP/6-311G(2d,d,p): $y = 0.960x + 0.055$, $R^2 = 0.983$. MPW1K/6-31G*: $y = 0.994x - 0.003$, $R^2 = 0.951$. MP2(Full)/6-31G*: $y = 1.289x - 0.712$, $R^2 = 0.771$.

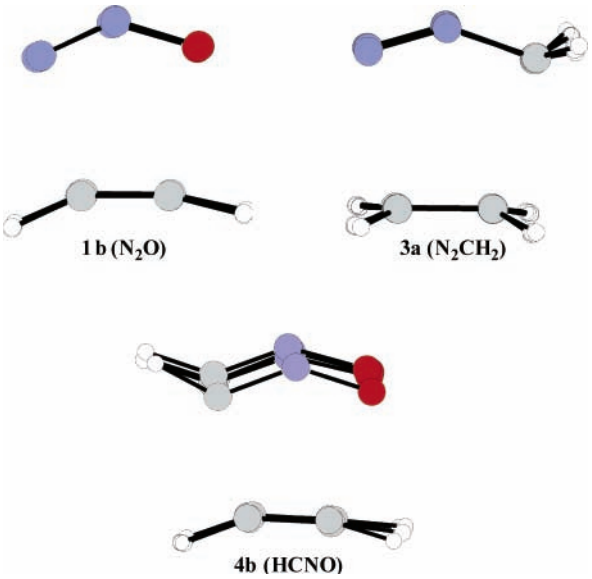

Figure 11. B3LYP/6-311G(2d,d,p), B3LYP/6-31G*, MPW1K/6-31G*, and MP2/6-31G* superimposed transition structures of reactions **1b**, **3a**, and **4b**.

(2d,d,p) and MPW1K. The reactions in least agreement are labeled in Figure 10.

To show that the computed structures for B3LYP, MPW1K, and MP2 are essentially the same, we superimposed the transition structures of reactions **1b**, **3a**, and **4b** (Figure 11). These reactions had computed transition structures that most deviated from B3LYP in Figure 10. The superimposed transition structures in Figure 11 show that all methods predict similar geometries with the only exception being the reaction of fulminic acid with acetylene, which shows that the MP2 method predicted shorter partial bond lengths than the DFT methods.

Revised Values of Experimental $\Delta H^{\ddagger}_{0K(exp)}$ for Hydrocarbon Pericyclic Reactions. A standard set of hydrocarbon pericyclic reactions was previously reported by Guner et al. for the benchmarking of quantum mechanical methods.[16,17] This has found use for the testing of new methods and functionals.[66−70] Figure 12 shows the 11 hydrocarbon pericyclic reactions. Examples of electrocyclic reactions (**hc1**−**hc3**), sigmatropic shifts (**hc4**−**hc6**), cycloadditions (**hc7**−**hc9**), and cycloreversions (**hc10** and **hc11**), are included. Previous estimation of activation enthalpies at 0 K were made from experimental activation enthalpies at finite temperatures, using computed thermal corrections (TCE) from frequency calculations on transition structures and reactants. However, several errors have been detected in the implementation of this procedure, so we have revised the estimated 0 K values that should be used for benchmarking. B3LYP/6-31G* thermal corrections computed at the reported experimental temperature have been subtracted from the best available experimental activation enthalpy values to estimate $\Delta H^{\ddagger}_{0K(exp)}$.

$$\Delta H^{\ddagger}_{0K(exp)} = (H^{\ddagger}_{T(exp)} - TCE_{TS}) - (H_{R(exp)} - TCE_{R})$$

It was previously shown that there is little method dependence

TABLE 6: Experimental Activation Enthalpies for Pericyclic Hydrocarbon Reactions hc1−hc11 Corrected to 0 K Using B3LYP/6-31G* Frequencies for Thermal Corrections

rxn	temp (K)	$\Delta H^{\ddagger}_{exp}$ (kcal/mol)	$\Delta H^{\ddagger}_{0K}$ (kcal/mol)
hc1	426	31.9[71] ± 0.2	31.9[a]
hc2	412	29.8[72] ± 0.5	30.2[a]
hc3	481	28.3[73] ± 0.3	28.1[b]
hc4	468	35.4[74] ± 0.5	36.8[a]
hc5	328	23.6[75] ± 0.5	23.7[a]
hc6	506	33.5[76] ± 0.5	34.5[a]
hc7	841	24.2[77] ± 2	25.0[b]
hc8	546	22.6[78] ± 1.6	23.7[b]
hc9	388	15.2[79−81] ± 0.6	15.9[b]
hc10	298	24.6[82] ± 3	24.3[a]
hc11	748	52.5[83,84] ± 3	51.6[b]

[a] Unchanged values from ref 16. [b] Revised estimated 0 K activation enthalpies.

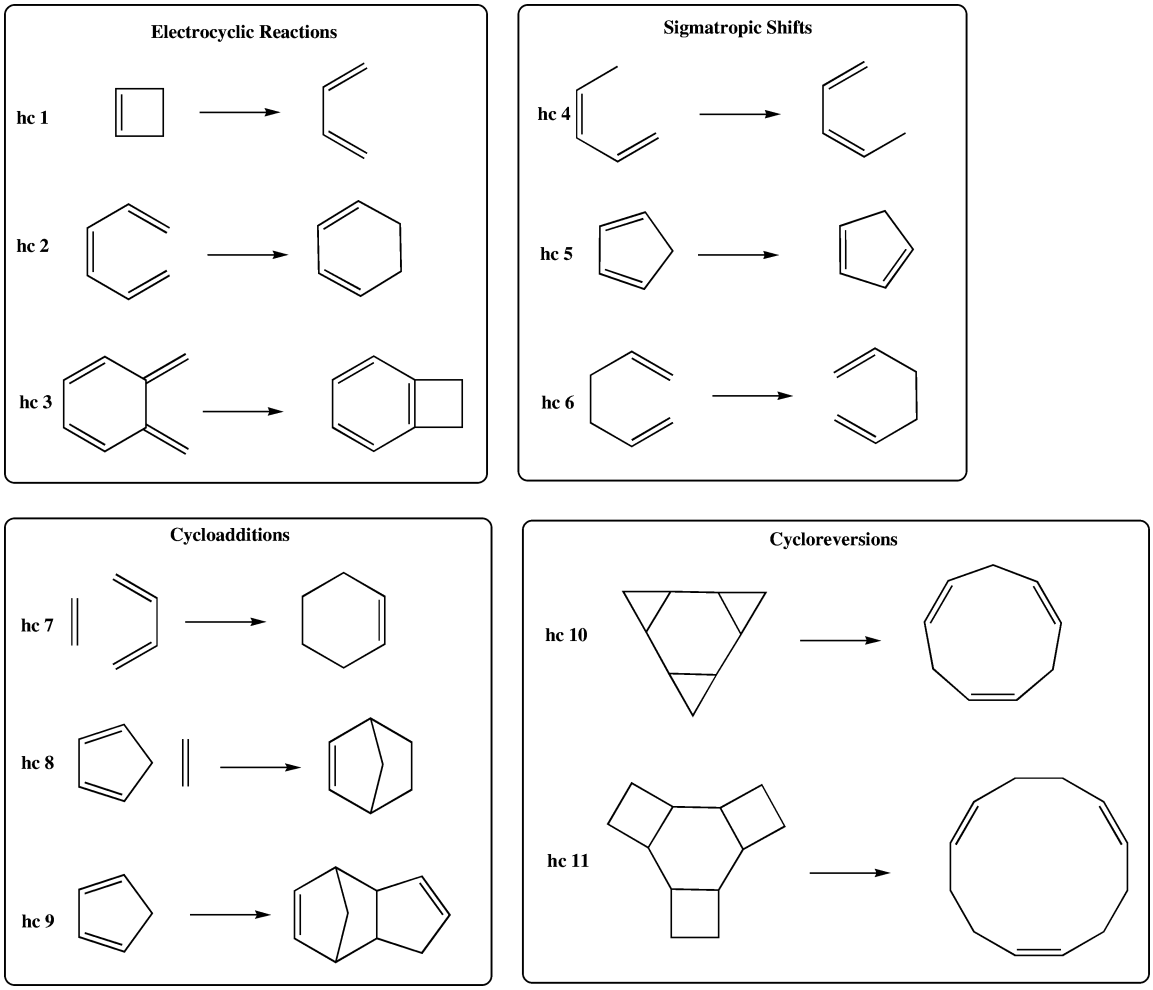

Figure 12. Standard set of hydrocarbon pericyclic reactions **hc1**−**hc11** used for the benchmarking of computational methods.

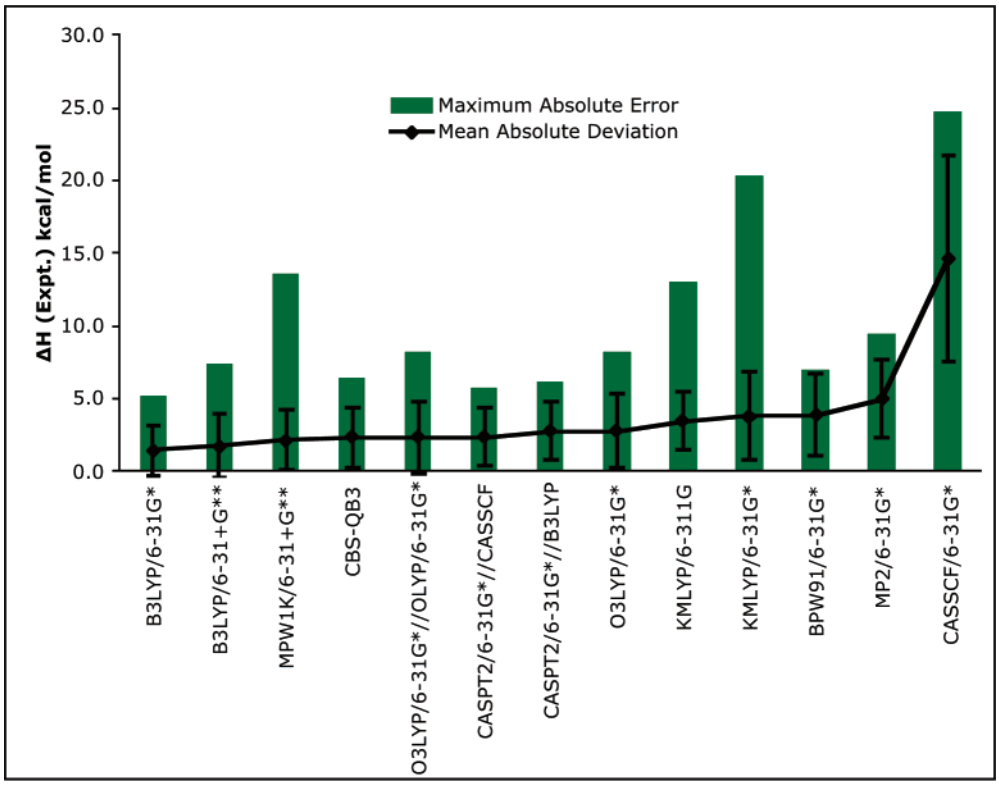

Figure 13. Deviation of DFT, post-Hartree−Fock, and multicomponent methods from experimental activation enthalpies at 0 K for hydrocarbon pericyclic reactions **hc1**−**hc9**. Error bars are standard deviations of the MAD values.

TABLE 7: Mean Deviations (MD), Mean Absolute Deviations (MAD), Standard Deviations (SD) of the MAD, and Maximum Negative and Positive Errors of Computed Activation at 0 K Relative to Experimental $\Delta H^{\ddagger}_{0K}$ Values for the Hydrocarbon Pericyclic Reactions 1−9[a]

method	MD	MAD	SD	max (−) error	max (+) error
B3LYP/6-31G*	0.8	1.5	1.7	2.3[c]	5.2[f]
B3LYP/6-31+G**	1.1	1.7	2.2	3.5[d]	7.3[f]
MPW1K/6-31+G**	1.1	2.1	2.1	3.1[c]	13.5[g]
CBS-QB3	−1.8	2.3	2.0	6.4[c]	2.1[h]
O3LYP/6-31G*//OLYP/6-31G*	0.9	2.4	2.5	3.2[d]	8.2[f]
CASPT2/6-31G*//CASSCF	−0.1	2.4	2.0	5.1[c]	5.7[h]
CASPT2/6-31G*//B3LYP	−0.5	2.8	2.0	6.1[c]	5.1[h]
O3LYP/6-31G*	−0.1	2.8	2.5	4.5[d]	8.2[g]
KMLYP/6-311G	1.9	3.5	1.9	4.6[c]	13.0[h]
KMLYP/6-31G*	1.3	3.8	3.0	6.5[c]	20.3[g]
BPW91/6-31G*	−3.7	3.9	2.8	6.9[e]	0.5[f]
MP2/6-31G*	−3.4	5.0	2.7	9.5[e]	3.9[g]
CASSCF/6-31G*	14.6	14.6	7.1	*b*	24.7[f]

[a] All values are in kcal/mol. [b] None of the activation enthalpies computed with CASSCF are lower than experimental values. [c] Diels−Alder reaction between cyclopentadiene and ethylene. [d] Ring closing of *o*-xylylene to benzocyclobutane. [e] Cope rearrangement of 1,5-hexadiene. [f] Dimerization of cyclopentadiene. [g] Ring opening of cyclobutene to butadiene. [h] 1,5-H shift of cyclopentadiene.

for computing thermal corrections. Table 6 lists the experimental temperatures that were used to compute the thermal corrections along with the updated estimated enthalpies of activation at 0 K.

The changes of $\Delta H^{\ddagger}_{0K}$ in this table from the previously published values are for reactions **hc3**, **hc7**−**hc9**, and **hc11**, for which incorrect values of 29.1, 23.3, 21.6, 15.1, and 46.5, respectively, were published previously.[16] Here we reevaluated DFT, ab initio, and multicomponent methods in comparison to the corrected set of 0 K activation enthalpies. Reactions **hc10** and **hc11** were not used in statistical evaluation of methods because of the low precision of the experimental values. Table 7 lists the MD, MAD, SD, and maximum errors. Again the top six methods all show good statistical agreement with experimental values. The most noteworthy change is the improvement of DFT methods. The O3LYP functional MAD decreased to 2.4 kcal/mol from the previously reported 3.0 kcal/mol.[17] Also important is that the MAD value of CBS-QB3 increased by about 1/2 kcal/mol to a value of 2.3 kcal/mol. As reported previously, even though the MAD values improve for DFT methods, the accurate CBS-QB3 and CASPT2 methods have lower maximum errors.[16] The only DFT functional that decreased in statistical accuracy with this reevaluation is the KMLYP method.

The corrected values show that most methods underestimated the barriers for the Diels−Alder reaction between cyclopentadiene and ethylene and the electrocyclic ring closure reaction of *o*-xylylene to benzocyclobutene. The deviations from experimental values are plotted in Figure 13.

Figure 14 compares computed and experimental activation barriers for the standard set of pericyclic reactions. Figure 15 compares the five most statistically accurate methods to the experimental values using a linear regression analysis. This reevaluation of methods shows that DFT methods tended to improve, while CBS-QB3 and CASPT2 performed worse in this analysis. However, CBS-QB3 and CASPT2 still show more linear slopes and better R^2 values. O3LYP showed improved MAD and MD values, but showed poorer correlation to experimental numbers with too low of a slope value and a bad R^2 value.

Conclusions

For the major classes of 1,3-dipolar cycloadditions, the MPW1K DFT method with the 6-31G* basis set gives computed

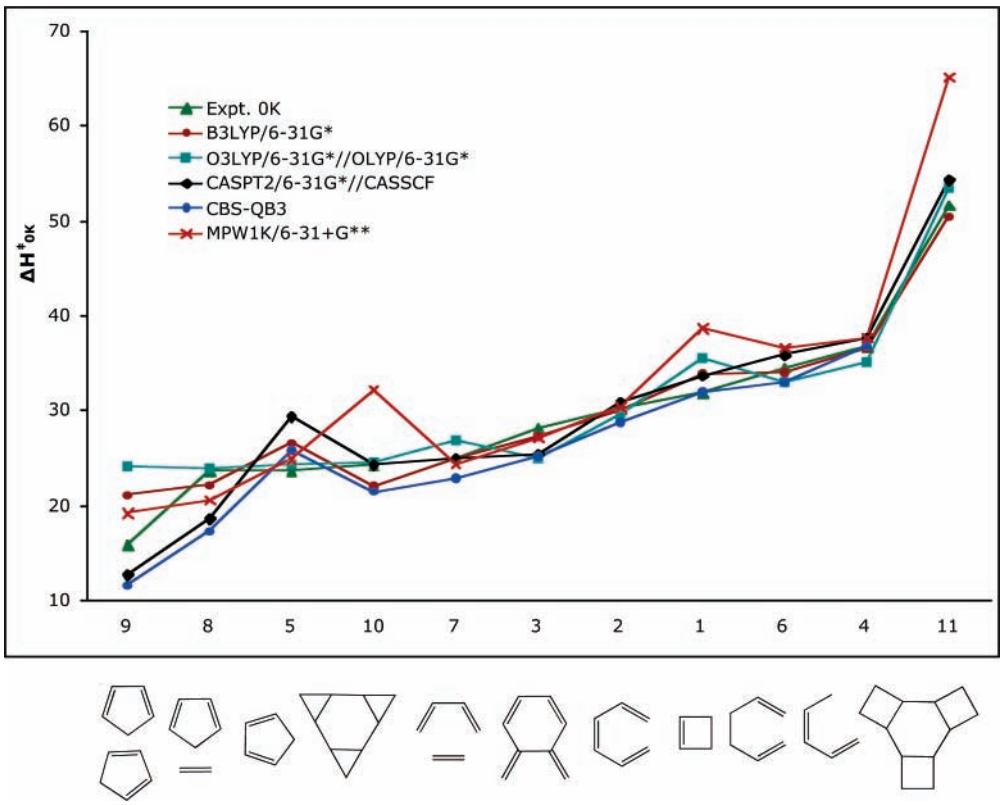

Figure 14. Experimental activation enthalpies compared to the best DFT, ab initio, and multicomponent methods for pericyclic reactions **hc1**−**hc11**.

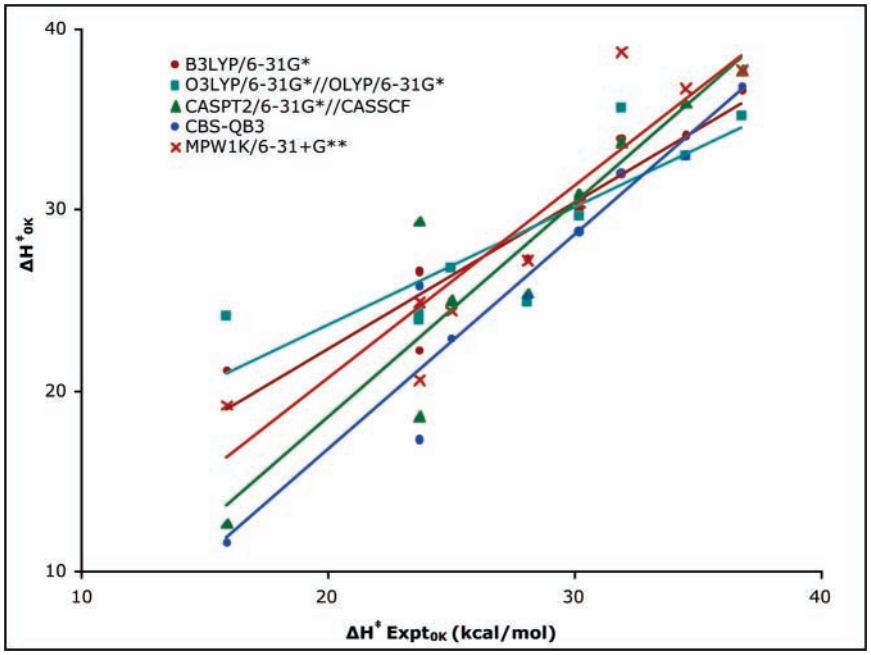

Figure 15. Plot of computed activation enthalpies at 0 K vs experimental activation enthalpies at 0 K for hydrocarbon pericyclic reactions **hc1**−**hc9**. A linear regression is also plotted. B3LYP/6-31G*: $y = 0.808x + 6.12$, $R^2 = 0.90$. O3LYP/6-31G*//OLYP/6-31G*: $y = 0.65x + 10.69$, $R^2 = 0.728$. CASPT2/6-31G*//CASSCF: $y = 1.185x - 5.189$, $R^2 = 0.867$. CBS-QB3: $y = 1.181x - 6.851$, $R^2 = 0.920$. MPW1K/6-31+G**: $y = 1.065x - 0.695$, $R^2 = 0.858$. $N = 9$ for all linear regressions.

activation enthalpies closest to those predicted by CBS-QB3. The B3LYP method performed best for reaction enthalpies, while MPW1K showed large error, due to being optimized for barrier heights. MP2 predicted much lower barriers than DFT methods, and the MAD is 2.3 kcal/mol higher than that for MPW1K. When the B3LYP and MPW1K methods were plotted versus CBS-QB3 values, MPW1K, as expected, correlated best. This analysis revealed that B3LYP had a systematic error of overestimating the activation enthalpy. MPW1K predicted barriers much closer to CBS-QB3 than B3LYP when comparing each class of dipolar cycloaddition. However, B3LYP and MPW1K predicted barriers with equal accuracy when compared by electronegative substitution of the dipole. Surprisingly, increasingly larger basis sets showed larger deviation from CBS-QB3 values. The 6-31G* basis set showed better performance than the recommended 6-31+G** for the MPW1K method. All DFT methods tested computed similar structures; only the MP2 method showed slight deviations in geometries. All computed transition structures showed a concerted synchronous pathway. Revised estimated 0 K experimental activation enthalpies for the standard set of pericyclic reactions showed DFT methods B3LYP and MPW1K improved in performance while the multicomponent CBS-QB3 decreased in accuracy compared to previously reported values.

Acknowledgment. We are grateful to the National Science Foundation for financial support of this research. This research was facilitated through the Partnerships for Advanced Computational Infrastructure (PACI) through the support of the National Science Foundation. The computations were performed on the National Science Foundation Terascale Computing System at the Pittsburgh Supercomputing Center (PSC) and on the UCLA Academic Technology Services (ATS) Hoffman Beowulf cluster. D.H.E. would like to acknowledge the NSF Integrative Graduate Education Research Traineeship program at UCLA for financial support.

Supporting Information Available: Cartesian coordinates and absolute energies for all 1,3-dipolar cycloaddition reactions. This material is available free of charge via the Internet at http://pubs.acs.org.

References and Notes

(1) *Quantum-Mechanical Prediction of Thermochemical Data*; Cioslowski, J., Ed.; Kluwer Academic Publishers: Boston, MA, 2001; Vol. 22, pp 1−245.
(2) Pople, J. A.; Head-Gordon, M.; Fox, D. J.; Raghavachari, K.; Curtiss, L. A. *J. Chem. Phys.* **1989**, *90*, 5622−5629.
(3) Curtiss, L. A.; Jones, C.; Trucks, G. W.; Raghavachari, K.; Pople, J. A. *J. Chem. Phys.* **1990**, *93*, 2537−2545.
(4) Curtiss, L. A.; Trucks, G. W.; Raghavachari, K.; Pople, J. A. *J. Chem. Phys.* **1991**, *94*, 7221−7230.
(5) Curtiss, L. A.; Raghavachari, K.; Redfern, P. C.; Rassolov, V.; Pople, J. A. *J. Chem. Phys.* **1998**, *109*, 7764−7776.
(6) Montgomery, J. A.; Frisch, M. J.; Ochterski, J. W.; Petersson, G. A. *J. Chem. Phys.* **1999**, *110*, 2822−2827.
(7) Nyden, M. R.; Petersson, G. A. *J. Chem. Phys.* **1981**, *75*, 1843−1862.
(8) Al-Laham, M. A.; Petersson, G. A. *J. Chem. Phys.* **1991**, *94*, 6081−6090.
(9) Petersson, G. A.; Tensfeldt, T. G.; Montgomery, J. A. *J. Chem. Phys.* **1991**, *94*, 6091−6101.
(10) Petersson, G. A.; Malick, D. K.; Wilson, W. G.; Ochterski, J. W.; Montgomery, J. A.; Frisch, M. J. *J. Chem. Phys.* **1998**, *109*, 10570−10579.
(11) Montgomery, J. A.; Frisch, M. J.; Ochterski, J. W.; Petersson, G. A. *J. Chem. Phys.* **2000**, *112*, 6532−6542.
(12) Martin, J. M. L.; Oliveria, G. *J. Chem. Phys.* **1999**, *111*, 1843−1856.
(13) *Recent Advances in Density Functional Methods*; Chong, D. P., Ed.; World Scientific: Singapore, 1997; Parts I and II.
(14) *Recent Advances in Density Functional Methods*; Barone, V., Bencini, A., Eds.; World Scientific: Singapore, 1999; Part III.
(15) Adamo, C.; di Matteo, A.; Barone, V. *Adv. Quantum Chem.* **1999**, *36*, 45−76.
(16) Guner, V.; Khuong, K. S.; Leach, A. G.; Lee, P. S.; Bartberger, M. D.; Houk, K. N. *J. Phys. Chem. A* **2003**, *107*, 11445−11459.
(17) Guner, V. A.; Khuong, K. S.; Houk, K. N.; Chuma, A.; Pulay, P. *J. Phys. Chem. A* **2004**, *108*, 2959−2965.
(18) Hariharan, P. C.; Pople, J. A. *Theor. Chim. Acta* **1973**, *28*, 213−222.
(19) Krishnan, R.; Binkley, J. S.; Seeger, R.; Pople, J. A. *J. Chem. Phys.* **1980**, *72*, 650−654.

(20) Frisch, M. J.; Pople, J. A.; Binkley, J. S. *J. Chem. Phys.* **1984**, *80*, 3265−3269.
(21) Clark, T.; Chandrasekhar, J.; Spitznagel, G. W.; Schleyer, P. v. R. *J. Comput. Chem.* **1983**, *4*, 294−301.
(22) Huisgen, R. *Angew. Chem., Int. Ed. Engl.* **1963**, *2*, 565−598.
(23) Huisgen, R. *Angew. Chem., Int. Ed. Engl.* **1963**, *2*, 633−645.
(24) Huisgen, R. *Angew. Chem., Int. Ed. Engl.* **1968**, *7*, 321−328.
(25) Huisgen, R. *J. Org. Chem.* **1968**, *33*, 2291−2297.
(26) Huisgen, R. *J. Org. Chem.* **1976**, *41*, 403−419.
(27) Huisgen, R. In *1,3-Dipolar Cycloaddition Chemistry*; Padwa, A., Ed.; John Wiley & Sons: New York, 1984; Vol. 1.
(28) Houk, K. N. In *1,3-Dipolar Cycloaddition Chemistry*; Padwa, A., Ed.; John Wiley & Sons: New York, 1984; Vol. 2.
(29) Houk, K. N. *J. Am. Chem. Soc.* **1972**, *94*, 8953−8955.
(30) Caramella, P.; Gandour, R. W.; Hall, J. A.; Deville, C. G.; Houk, K. N. *J. Am. Chem. Soc.* **1977**, *99*, 385−392.
(31) Caramella, P.; Houk, K. N. *J. Am. Chem. Soc.* **1976**, *98*, 6397−6399.
(32) Houk, K.N.; Sims, J. *J. Am. Chem. Soc.* **1973**, *95*, 5798−5800.
(33) Houk, K. N.; Sims, J.; Duke, R. E., Jr.; Strozier, R. W.; George, J. K. *J. Am. Chem. Soc.* **1973**, *95*, 7287−7301.
(34) Houk, K. N.; Sims, J.; Watts, C. R.; Luskus, L. J. *J. Am. Chem. Soc.* **1973**, *95*, 7301−7315.
(35) Houk, K. N. *Acc. Chem. Res.* **1975**, *8*, 361−369.
(36) Poppinger, D. *J. Am. Chem. Soc.* **1975**, *97*, 7486−7488.
(37) Caramella, P.; Houk, K. N.; Domelsmith, L. N. *J. Am. Chem. Soc.* **1977**, *99*, 4511−4514.
(38) Dewar, M. J. S.; Olivella, S.; Rzepa, H. S. *J. Am. Chem. Soc.* **1973**, *100*, 5650−5659.
(39) Su, M.; Liao, H.; Chung, W.; Chu, S. *J. Org. Chem.* **1999**, *64*, 6710−6716.
(40) Confalone, P. N.; Huie, E. M. *Org. React. (N.Y.)* **1988**, *36*, 1.
(41) Sustmann, R.; Wenning, E. *Tetrahedron Lett.* **1977**, *10*, 877−880.
(42) Sustmann, R. *Tetrahedron Lett.* **1971**, *12*, 2717−2720.
(43) Goddard, W. A., III; Dunning, T. H., Jr.; Hunt, W. J.; Hay, P. J. *Acc. Chem. Res.* **1973**, *6*, 368−376.
(44) Yamaguchi, K.; Nishio, A.; Yabushita, S.; Fueno, T. *Chem. Phys. Lett.* **1978**, *53*, 109−114.
(45) Yamaguchi, K.; Yabushita, S.; Fueno, T.; Kato, S.; Morokuma, K.; Iwata, S. *Chem. Phys. Lett.* **1980**, *71*, 563−568.
(46) Hiberty, P. C.; Ohanessian, G. *J. Am. Chem. Soc.* **1982**, *104*, 66−70.
(47) Firestone, R. A. *J. Org. Chem.* **1968**, *33*, 2285−2290.
(48) Firestone, R. A. *J. Org. Chem.* **1968**, *37*, 2181−2191.
(49) Firestone, R. A. *Tetrahedron* **1977**, *33*, 3009−3039.
(50) Hiberty, P. C.; Ohanessian, G.; Schlegel, H. B. *J. Am. Chem. Soc.* **1983**, *105*, 719−723.
(51) Kohn, W.; Sham, L. J. *Phys. Rev.* **1965**, *140*, A1133−A1138.
(52) Hohenberg, P.; Kohn, W. *Phys. Rev.* **1965**, *136*, B864−B871.
(53) Becke, A. D. *J. Chem. Phys.* **1993**, *98*, 5648−5652.
(54) Stephens, P. J.; Devlin, F. J.; Chabalowski, C. F.; Frisch, M. J. *J. Chem. Phys.* **1994**, *98*, 11623−11627.
(55) Adamo, C.; Barone, V. *J. Chem. Phys.* **1998**, *108*, 664−675.
(56) Lynch, B. J.; Fast, P. L.; Harris, M.; Truhlar, D. G. *J. Phys. Chem. A* **2000**, *104*, 4811−4815.
(57) Lynch, B. J.; Zhao, Y.; Truhlar, D. G. *J. Phys. Chem. A* **2003**, *107*, 1384−1388.
(58) Lynch, B. J.; Truhlar, D. G. *J. Phys. Chem. A* **2001**, *105*, 2936−2941.
(59) Lynch, B. J.; Truhlar, D. G. *J. Phys. Chem. A* **2002**, *106*, 842−846.
(60) Lynch, B. J.; Truhlar, D. G. *J. Phys. Chem. A* **2003**, *107*, 3898−3906.
(61) Frisch, M. J.; et al. *Gaussian 98*, revision A.9; Gaussian, Inc.: Pittsburgh, PA, 1998.
(62) Frisch, M. J.; et al. *Gaussian 03*, revision C.02; Gaussian, Inc.: Wallingford, CT, 2004.
(63) Geittner, J.; Huisgen, R.; Reissig, H. U. *Heterocycles* **1978**, 109.
(64) Møller, C.; Plesset, M. S. *Phys. Rev.* **1934**, *46*, 618.
(65) Head-Gordon, M.; Pople, J. A.; Frisch, M. J. *Chem. Phys. Lett.* **1988**, *153*, 503−506.
(66) Boese, A. D.; Martin, J. M. L. *J. Chem. Phys.* **2004**, *121*, 3405−3416.
(67) Sancho-Garcia, J. C.; Cornil, J. *J. Chem. Phys.* **2004**, *121*, 3096−3101.
(68) Gherman, B. F.; Lippard, S. J.; Friesner, R. A. *J. Am. Chem. Soc.* **2005**, *127*, 1025−1037.
(69) Alajarin, M.; Sanchez-Andrada, P.; Vidal, A.; Tovar, F. *J. Org. Chem.* **2005**, *70*, 1340−1349.
(70) Goumans, T. P. M.; Ehlers, A. W.; Lammertsma, K.; Wuerthwein, E.-U.; Grimme, S. *Chem.—Eur. J.* **2004**, *10*, 6468−6475.
(71) Hauser, W. P.; Walters, W. D. *J. Phys. Chem.* **1968**, *67*, 1328−1333.
(72) Lewis, K. E.; Steiner, H. *J. Chem. Soc.* **1964**, 3080.
(73) Roth, W. R.; Biermann, M.; Dekker, H.; Jochems, R.; Mosselman, C.; Herman, H. *Chem. Ber.* **1978**, *111*, 3892−3903.
(74) Roth, W. R. *Chimia* **1966**, *229*, 20.
(75) Roth, W. R. *Tetrahedron Lett.* **1964**, 1009−1013.
(76) Doering, W. E.; Toscano, V. G.; Beasley, G. H. *Tetrahedron* **1971**, *27*, 5299−5306.
(77) Rowley, D.; Steiner, H. *Discuss. Faraday Soc.* **1951**, *27*, 5299−5306.
(78) Walls, R.; Wells, J. M. *J. Chem. Soc., Perkin Trans. 2* **1976**, 52−55.
(79) Benford, G. A.; Wassermann, A. *J. Chem. Soc.* **1939**, *362*, 367−371.
(80) Turnbull, A. G.; Hull, H. S. *Aust. J. Chem.* **1968**, *21*, 1789−1797.
(81) Herndon, W. C.; Grayson, C. R.; Manion, J. M. *J. Org. Chem.* **1967**, *32*, 526−529.
(82) Spielman, W.; Fick, H. H.; Meyer, L. U.; de Meijere, A. *Tetrahedron Lett.* **1976**, *45*, 4057.
(83) Maas, M.; Lutterbeck, M.; Hunkler, D.; Prinzbach, H. *Tetrahedron Lett.* **1983**, *24*, 2143−2149.
(84) Mohler, D. L.; Vollhardt, R. P. C.; Wolf, S. *Angew. Chem., Int. Ed. Engl.* **1990**, *29*, 1151−1154.